CHARACTERIZATION OF THE NUCLEAR ENVELOPE, PORE COMPLEXES, AND DENSE LAMINA OF MOUSE LIVER NUCLEI BY HIGH RESOLUTION SCANNING ELECTRON MICROSCOPY

ROBERT H. KIRSCHNER, MICHAEL RUSLI, and TERENCE E. MARTIN

From the Department of Pathology and the Whitman Laboratory, Department of Biology, University of Chicago, Chicago, Illinois 60637

ABSTRACT

We have used high resolution scanning electron microscopy (SEM) to study the nuclear envelope components of isolated mouse liver nuclei. The surfaces of intact nuclei are covered by closely packed ribosomes which are distinguishable by SEM from nuclear pore complexes. After removal of nuclear membranes with the nonionic detergent Triton X-100, the pore complexes remain attached to an underlying, peripheral nuclear lamina, as described by others. The surface of this dense lamina is composed of particulate granules, 75–150 Å in diameter, which are contiguous over the entire periphery. We did not observe the pore-to-pore fibril network suggested by other investigators, but such a structure might be the framework upon which the dense lamina is formed. Morphometric analysis of pores and pore complexes shows their size, structure, and density to be similar to that of other mammalian cells. In addition, several types of pore complex-associated structures, not previously reported by other electron microscope (EM) techniques, are observed by SEM. Our studies suggest that the major role of the dense lamina is associated with the distribution, stability, and perhaps, biogenesis of nuclear pore complexes. Treatment of isolated nuclei with a combination of Triton X-100 and sodium deoxycholate removes membranes, dense lamina, and nuclear pore complexes. The resulting "chromatin nuclei" retain their integrity despite the absence of any limiting peripheral structures.

Despite the attention devoted to the nuclear envelope, our knowledge of the organization, function, and biogenesis of this complex membrane system is still incomplete. There is sufficient experimental evidence to suggest its role in nuclear-cytoplasmic exchange (39, 40, 45) and in the organization of interphase chromatin (see references 12, 14, 17, 25, 44, and 50 for recent reviews) but the mechanisms involved are poorly understood. In part, this is due to a lack of certainty about the structure and interrelationships of the various envelope components to each other and to the underlying chromatin and associated nucleoplasmic substances. For example, current methods of exploring the morphological relationship of nuclear pores to outer membrane ribosomes require extrapolation of data from either multiple thin sections (13, 24) or from freeze-etched sections (49) to reconstruct surface topography. Unfortunately, freeze-cleaving produces uncertain fracture planes, and heavy

metal replicas of the nuclear surface fail to clearly reveal either ribosome or pore complex structure (47, 49). Thus, there has been little progress in our understanding of the organization of these envelope-associated ribosomes since their relationship to the annuli of the nuclear pore complexes was first proposed by Swift (46), nearly 20 years ago.

From the early studies of Gall (18, 19) and of Watson (48) onward, electron microscopy has shown remarkable similarity of nuclear-pore-complex architecture in a variety of species (9, 13, 15, 20, 22, 31); but the morphology and morphometry of the envelope, nuclear pores, and pore complexes may vary depending upon the preparative techniques used (13, 19, 22, 30, 35). Indeed, the controversy surrounding the preferential removal by detergents (e.g. 23, 38) or other agents (e.g. 43) of the outer nuclear membrane has been, in part, due to the difficulty of distinguishing between inner nuclear membrane and the nonmembranous "fibrous" or "dense" lamina, described by Fawcett (11), and observed at the periphery of the chromatin in many cell types (1, 2, 5, 41). The concept of pore complexes as distinct cellular organelles (3, 10) has evolved concurrent with evidence that they remain attached to the lamina at the nuclear periphery after complete removal of the nuclear membranes (1, 5); that they can be observed as isolated, intact, ring structures containing annular subunits in preparations of fragmented nuclear membranes (from oocytes of the newt *Taricha granulosa* (10; see also 9, 15, and 16)); and that they can be isolated in association with a 150-Å thick, perichromatin lamina from rat liver nuclei (1, 2). Similar nonmembranous components of mammalian cell nuclei, identified as "nuclear protein matrix" (6) or "nuclear ghosts" (26, 37), have been isolated by various sequential detergent and salt extractions. Other evidence from amphibian oocytes as well as rat liver cells suggests an "intrinsic membrane component ... (that) constitute(s) a detergent-resistant interpore skeleton network" (39). Although several apparently identical major protein fractions have been identified in such preparations (2, 6, 26, 37, 42), there are significant structural (2, 6, 26, 40) and biochemical (26) differences present. To gain a different perspective of the nuclear envelope, we have used high resolution scanning electron microscopy to study the surface architecture of isolated mouse liver nuclei and the alterations that occur in the nuclear membranes and dense lamina after treatment with nonionic and ionic detergents.

MATERIALS AND METHODS

Isolation of Nuclei

Mouse liver nuclei from CFW mice were prepared according to a modification of the method of Chauveau et al (7). Finely minced liver tissue in 2 vol cold 0.25 M sucrose, 0.005 M Tris HCl, 0.008 M KCl, 0.0015 M $MgCl_2$, pH 7.6 (sucrose-TKM buffer) was homogenized by hand with a Dounce homogenizer (Kontes Co., Vineland, N. J.). The homogenate was then diluted with 2 vol 2.0 M sucrose-TKM buffer and gently layered onto 4-ml cushions of 2.0 M sucrose-TKM buffer in polycarbonate centrifuge tubes. The samples were centrifuged in an L2-65 preparative ultracentrifuge (Beckman Instruments, Inc., Spinco Div., Palo Alto, Calif.) using a type 50 Ti rotor at 40,000 rpm for 40 min. After centrifugation, the pelleted nuclei were resuspended in 0.25 M sucrose-TKM buffer to a final concentration of 1.0×10^5/ml, and the preparation was checked for purity by phase-contrast microscopy.

Treatment of Nuclei with Detergents

Nuclear membranes were removed by the addition of cold 10% Triton X-100 or a mixture of 10% Triton and 10% sodium deoxycholate (both from Sigma Chemical Co., St. Louis, Mo.) to a final concentration of 1% in the nuclear suspension. Nuclei were incubated for 90 s at 4°C, and the reaction was stopped by the addition of 2 vol glutaraldehyde fixative.

Sample Preparation for Scanning Electron Microscopy (SEM)

All samples were prepared in triplicate. Formvar-coated aluminum support disks, 0.8 cm diameter, were placed on moist filter paper in plastic petri dishes. Using a Pasteur pipette, one drop (approximately 25 μl) of resuspended nuclei at 4°C was placed on each of the three disks and allowed to settle for 2–3 min. The samples were then fixed by adding two drops (50 μl) of cold 2% glutaraldehyde-0.1 M Na-cacodylate buffer (pH 7.4; 300 mosmol) to each disk. Immediately, glutaraldehyde and the sample suspension were gently intermixed to promote rapid fixation. Detergent-treated nuclei were placed on support disks as soon as detergent had been added to the suspension, and after 90 s incubation the fixative was added. The petri dishes were then tightly sealed and samples were fixed, undisturbed, from 4 to 24 h at 4°C.

After fixation, samples were dehydrated serially (30 s, each step) through a graded series of ethanol solutions (10, 30, 50, 70, 80, 90, 95%) to 100% ethanol and dried at the critical point of CO_2 (4) in a Bomar SPC-50/EX apparatus (The Bomar Co., Tacoma, Wash.). Speci-

mens were shadowed in an Edwards 306 vacuum evaporator (Edwards High Vacuum, Inc., Grand Island, N. Y.) using gold-palladium wire (60% Au-40% Pd, 8 m diameter) at a vacuum of 10^{-6} Torr applied from a distance of 10 cm at an angle of 45°. Exactly 6.5 cm of the metal was evaporated from a tungsten wire over a period of 10 min while the specimens rotated on a rotary-tilt stage. This produced a coat 50–60 Å thick and a shadow grain not apparent at × 100,000.

Sample Preparation for Transmission Electron Microscopy (TEM)

For each specimen prepared for SEM, another fraction of the same sample was mixed with 2 vol of glutaraldehyde, centrifuged to form a pellet, and fixed for 24 h. These samples were postfixed for 30 min in 1% osmium tetroxide (OsO_4)-collidine buffer, pH 7.4, dehydrated through a graded series of ethanol solutions, embedded in Epon, sectioned, and stained with lead citrate and uranyl acetate.

To determine the coating thickness of SEM specimens, representative samples were scraped from SEM support disks and deposited in the tips of embedding capsules. Samples were embedded directly in Epon, sectioned, and examined in the TEM without further staining.

Electron Microscopy

Specimens prepared for SEM were examined in a Hitachi HFS-2 scanning electron microscope operated at 25 kV with an emission current of 1.5–2.0 μA, at a vacuum of 5×10^{-8} Torr (28, 29). Samples were examined at magnifications ranging from 10,000 to 100,000 with a routinely obtainable point-to-point resolution of 30 Å.

TEM was performed using a Philips 201 electron microscope operated at 80 kV. Fractions of all samples prepared for SEM were examined by conventional TEM as an aid to interpretation of membrane components visualized in the SEM.

Nuclear Morphometry

Nuclear diameters were determined by light microscopy using a filar micrometer eyepiece (American Optical Corp., Buffalo, N. Y.) fitted to a phase-contrast microscope. Freshly isolated nuclei, glutaraldehyde-fixed nuclei, and ethanol-dehydrated nuclei were measured in suspension. To measure critical point-dried nuclei, samples prepared on Formvar-coated glass discs were processed along with routine SEM samples on aluminum disks. After Au-Pd shadowing, cover slips were mounted using Permount (Fisher Scientific Co., Pittsburgh, Pa.) and the nuclear diameters were determined with the micrometer eyepiece at a magnification of 450.

Measurements of ribosome size, nuclear pore size, and pore complex size were made from SEMs at an original magnification of 50,000. Determinations of pore density were made from low magnification (× 15,000) micrographs encompassing the entire nucleus. The negatives were enlarged to three times their original magnification (× 150,000 and × 45,000) before being analyzed. In the calculations of pore density, the area of the convex surface of the nucleus (A_c) in which pores could be counted was determined by the formula

$$A_c = 2\pi r_1 h, \tag{1}$$

where r_1 = radius of the nucleus and h = height of the segment being measured. The height of the segment is determined as follows:

$$h = r_1 - x, \tag{2}$$

where

$$x = \sqrt{r_1^2 - r_2^2}, \tag{3}$$

and r_2 = radius of the segment being measured; r_1 and r_2 form the hypotenuse and one leg, respectively, of a right triangle. The geometrical basis of the formula is illustrated in Fig. 1.

RESULTS

Intact Nuclei

Isolated mouse liver nuclei prepared for SEM retain a spherical shape and intact nuclear enve-

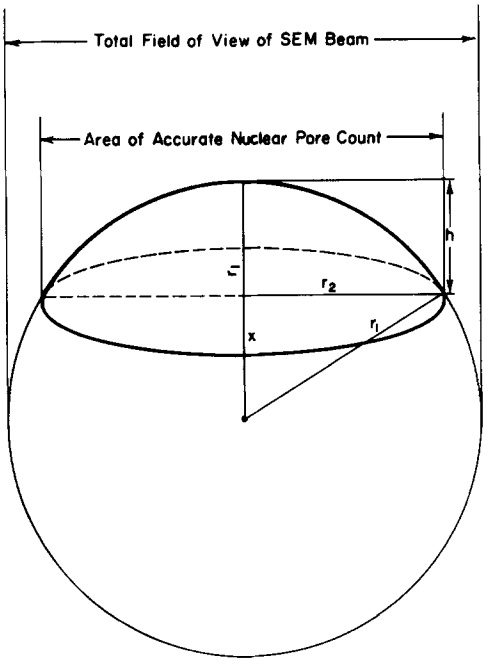

FIGURE 1 Calculation of the surface area of a convex segment of a sphere (nucleus); the radii r_1 and r_2 are determined by measuring photographic enlargements of nuclei.

lope. At low magnification (Fig. 2) the surfaces have a finely granular appearance interrupted by variable numbers of outer membrane blebs and adherent fragments of cytoplasmic membranes. In some nuclei, areas of increased backscattering of electrons from internal dense areas, such as nucleoli or heterochromatin, are seen. The granular appearance of the nuclei represents the blanket of ribosomes adherent to the outer nuclear membrane, among which nuclear pores are scattered (Fig. 3*a*). In most nuclei the ribosomes cover the entire surface. In about 3% of nuclei, however, there are areas of nuclear membrane that appear free of ribosomes, as in Fig. 3*a*. In such nuclei, nuclear pore complexes remain contiguous with ribosomes and few nuclear pores are seen in areas devoid of them. These smooth membrane areas either lacked ribosomes *in situ* or are regions from which ribosomes were stripped during organelle preparation. We can not exclude the possibility that in these regions the outer nuclear membrane has been removed exposing the inner nuclear membrane, but this seems less likely since, in our experience, disrupted membranes are easily recognized in the SEM. Particles interpreted as individual ribosomes have diameters of 200–250 Å with center-to-center distances of about 300 Å, in agreement with results obtained using other techniques (36). We cannot determine whether these ribosomes are linked into polyribosome chains but they are frequently grouped in patterns suggestive of such an association (Fig. 4 and reference 27).

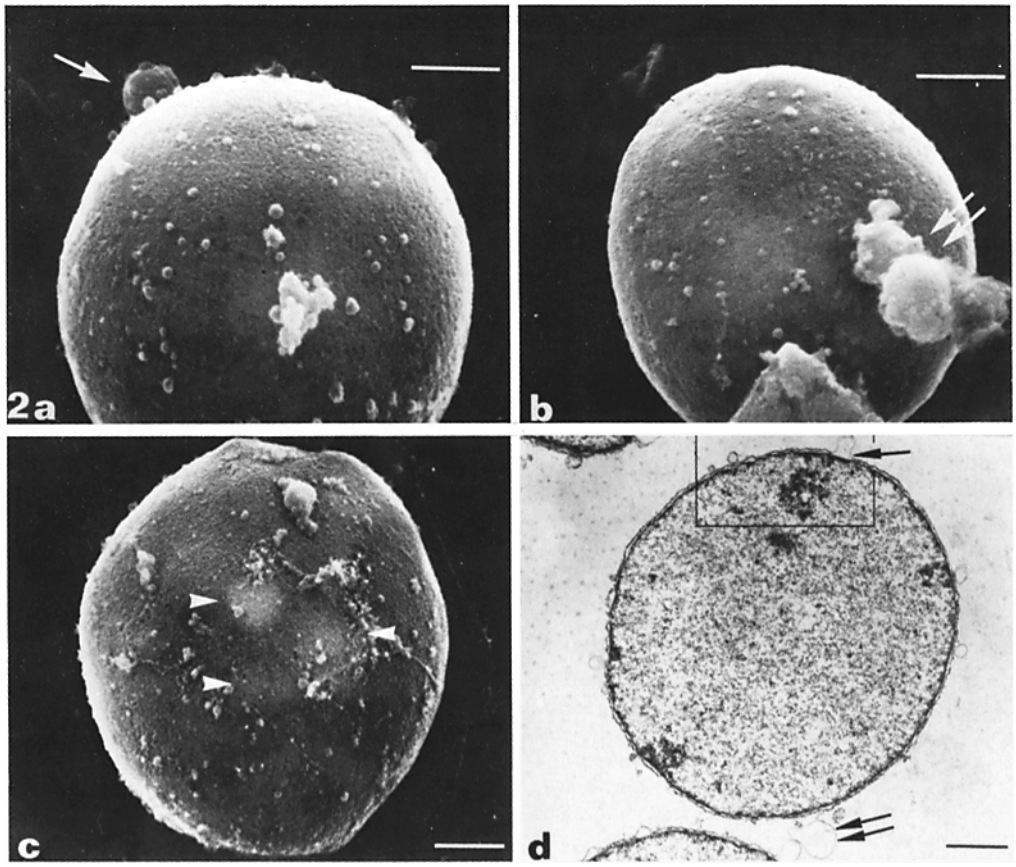

FIGURE 2 SEMs of isolated mouse liver nuclei (*a, b, c*). The fine, granular surfaces reflect the closely packed blanket of ribosomes present on each nucleus. Outer membrane blebs (↑) and attached fragments of cytoplasmic membrane (↑ ↑) can be identified. Three areas of increased backscattering of electrons from internal dense areas (▲) are seen (*c*). Transmission microscopy (*d*) shows similar outer membrane blebs and adherent microsomal membrane. Bar, 1.0 μm; 2*a, b,* × 12,000; *c*, × 9,000; *d*, × 8,000.

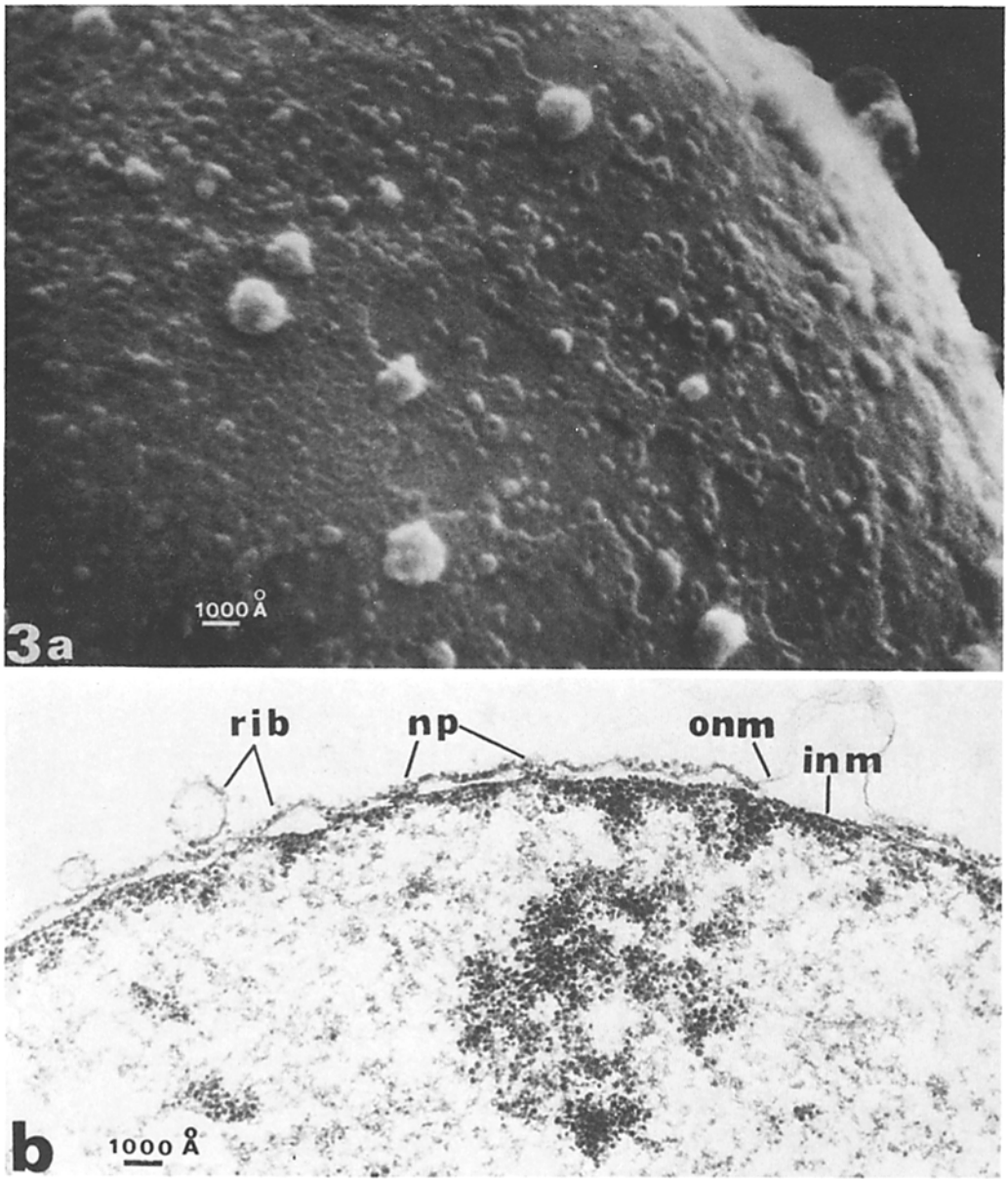

FIGURE 3 In (*a*), the nuclear pores, pore complexes, and areas of nuclear surface covered by ribosomes are clearly distinguished by SEM from those areas of the outer membrane devoid of ribosomes. Most pore complexes are surrounded by or contiguous to ribosomes. In an enlargement of portion of Fig. 2*d*, correlative TEM (*b*) corroborates the scanning microscopy images of ribosomes, pores, nuclear membrane blebs, and adherent cytoplasmic particles. *rib* = ribosome; *onm* = outer nuclear membrane; *inm* = inner membrane; *np* = nuclear pore. Fig. 3*a*, × 52,000; *b*, × 50,000.

Nuclear pore complexes are distinguishable from the surrounding ribosomes by the larger size of the annular subunits (Fig. 4*a*, *b*). The outside diameter of most nuclear pore complexes is approximately 850 Å with each annular subunit measuring approximately 300 Å in diameter; the central pores have a diameter of approximately 250 Å. The nuclear pores show clustering

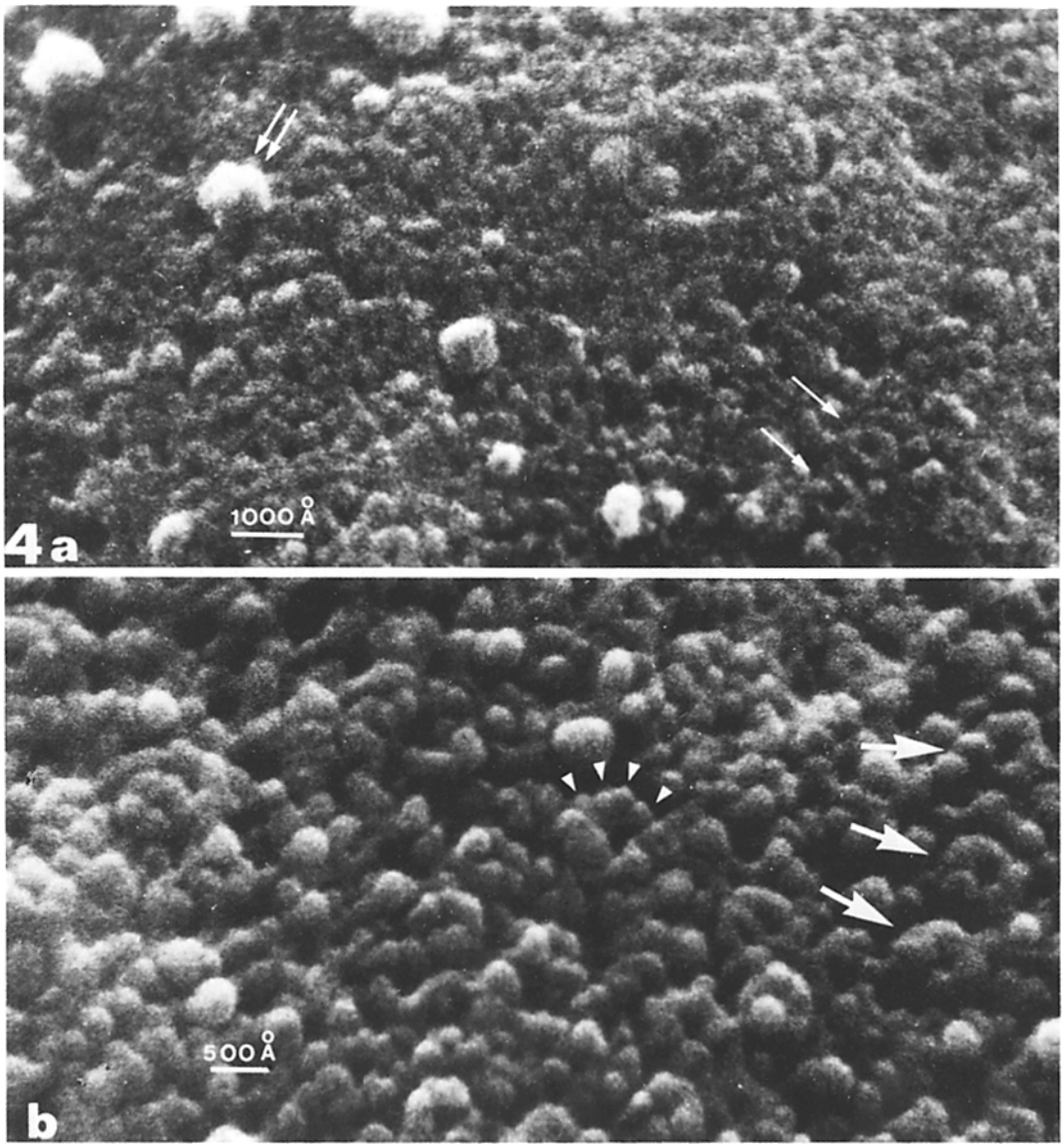

FIGURE 4 The surface of two nuclei at increasing magnification. In Fig. 4*a*, adherent cytoplasmic membranes (↑ ↑), ribosomes, and pore complexes (↑) are evident. In Fig. 4*b*, one can distinguish annular subunit structure in several nuclear pore complexes (↑). Individual ribosomes can also be discerned (▲), some of which form chains of length and configuration consistent with polysomes. Fig. 4*a*, × 107,000; *b*, × 150,000.

in groups of two to four pores each, but this is more obvious in Triton-treated nuclei, as discussed below. TEM of isolated nuclei (Fig. 3*b*) correlates well with the SEM and confirms the absence of any significant architectual artifact peculiar to SEM preparation.

When 50 each of freshly isolated, glutaraldehyde-fixed, ethanol-dehydrated, and critical point-dried nuclei were measured by light microscopy at a magnification of 450, the mean diameter of the freshly isolated nuclei (7.6 ± 1.1 μm) was not significantly altered by glutaraldehyde fixation (mean = 7.5 ± 0.9 μm) or ethanol dehydration (mean = 7.4 ± 0.7 μm). After criti-

cal point drying, however, the mean diameter of the nuclei was reduced by 26% to 5.6 ± 0.7 μm, reducing the surface area by 46%. Similar results were obtained with Triton-treated nuclei. When critical point-dried nuclei were removed from their SEM support disks, embedded, sectioned, and stained for TEM, the lack of significant architectual alteration was confirmed. Thus, the shrinkage produced by critical point drying appears to be a uniform miniaturization of the nuclei which preserves the usual organelle substructure.

Removal of Nuclear Membranes with Triton X-100

Treatment with the nonionic detergent Triton X-100 for 90 s effectively removes the inner and outer nuclear membranes, leaving the lamina and attached nuclear pore complexes intact (1, 2, 5). The pore complexes, which previously had been partially concealed by the nuclear membranes and associated ribosomes, are now prominent, and the clustering of the pores into small groups is evident (Figs. 5, 6). Annular subunits of many

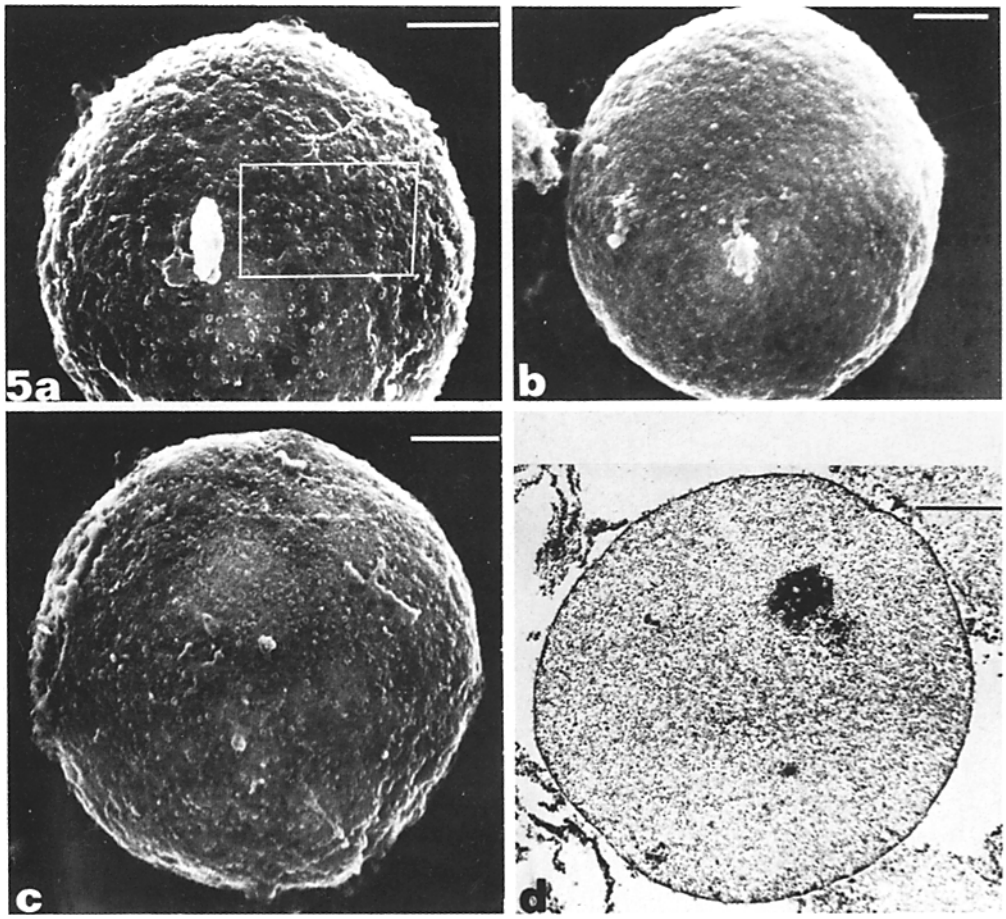

FIGURE 5 Representative nuclei incubated with the nonionic detergent Triton X-100 for 90 s (*a-c*). Nuclei are devoid of inner and outer nuclear membranes, revealing nuclear pore complexes and the dense lamina to which they are attached. The rectangular area in Fig. 5*a* is shown in greater detail in Fig. 6*a*. A TEM nuclear profile (*d*) from a sample prepared at the same time shows nuclear contents to be intact and limited by the dense lamina. Nuclear pore complexes are clearly visible. Bar, 1.0 μm; Figs. 5*a*, *c*, *d*, × 12,000; *b*, × 10,000.

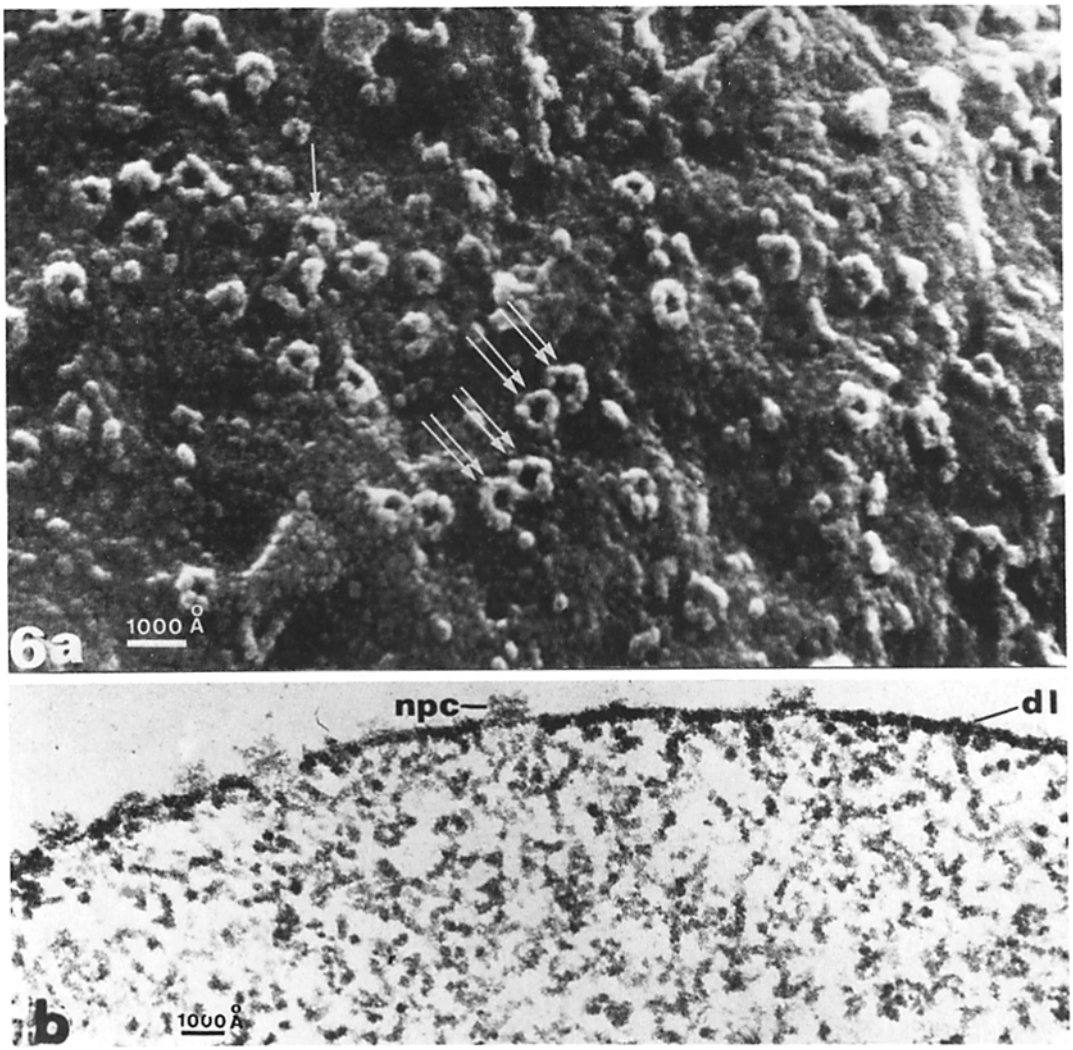

FIGURE 6 Surface detail of Triton-treated nucleus (*a*). Nuclear pore complexes are prominent, and in some (↑) eight subunits can be discerned. In others, there is a distinct cleavage between some subunits but not between all. A few nuclear pore complexes seem to share a common subunit (↑ ↑). Infrequent "pores" in the dense lamina not surrounded by annuli are also seen. TEM (*b*) shows nuclear pore complexes interspersed on the dense lamina, and the granular characteristics of the lamina. *npc* = nuclear pore complex; *dl* = dense lamina; Fig. 6*a*, × 80,000; *b*, × 58,000.

of the pores are clearly visible as globular particles (Figs. 6, 7). Markham rotational analysis (not shown) confirmed a strong four- and eight-fold symmetry for the pore complexes, and a paired arrangement of the annular subunits is suggested by their orientation in some of the complexes (Fig. 7*i*). Some pores are contiguous and others may share a common annular subunit (Fig. 6). Many particles having the size and shape of annular subunits extend from the pore complexes as varying length "chains", a few of which are of greater length than the circumference of the pore complexes. In some areas two pore complexes appear to be joined, or nearly joined, by such a "chain" (Fig. 7*a*, *b*, and *c*). Similar particles not directly associated with pore complexes but resting on the lamina are also seen (Fig. 7*k*). Occasional pits in the lamina, measur-

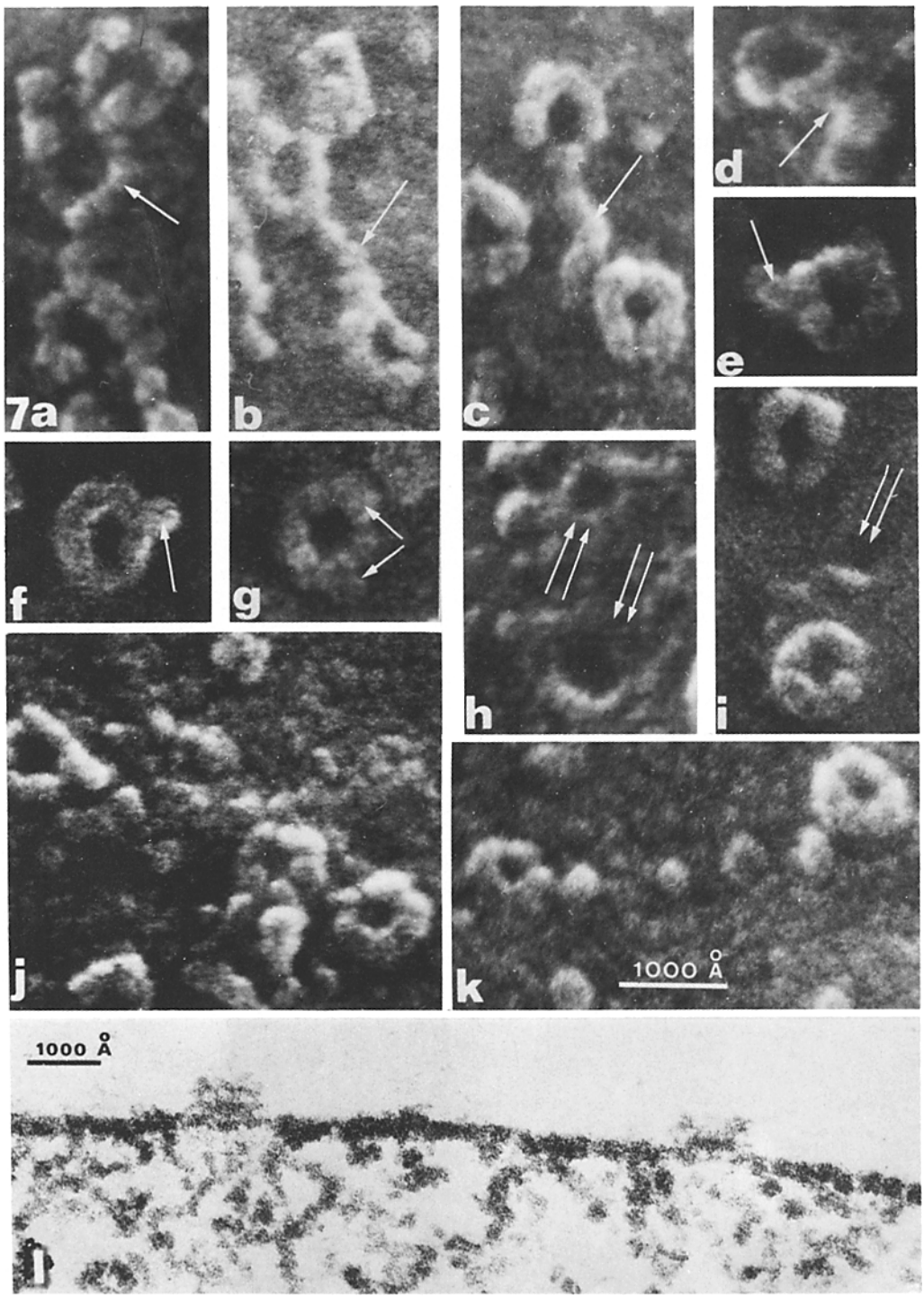

FIGURE 7 Individual nuclear pore complexes showing varying length "tails" (↑) extending from the pore complex and apparently composed of subunits similar in size and appearance. In some cases (*a*) the tails are longer than the circumference of the pore complex itself. Two pore complexes may be joined by such a strand (*b*), or nearly joined (*c*). Pores in the dense lamina without surrounding annuli (↑ ↑) are also seen (*h, i*). Note also the strong fourfold symmetry of the pore complexes in 7*i*. The granularity of the lamina is seen in 7*j, k* and shows granules of approximately 75–150 Å diam. A sectioned nucleus (*l*) clearly shows the granularity of the dense lamina and profiles of two nuclear pore complexes. Fig. 7*a–k*, × 160,000; *l*, × 108,000.

ing approximately 400 Å in diameter (Fig. 7*h, i*), may represent nuclear pores from which the annular complexes had been stripped during detergent treatment. At higher magnifications the granularity of the lamina is readily apparent. There is a pebble-grain pattern containing closely packed "granules" 75–150 Å in diameter, which corresponds to the appearance and dimensions of the dense lamina in thin section (Figs. 6*b*, 7*l*). Structures that might represent the pore-to-pore fibril network described by other investigators (10, 15, 26, 41) in isolated nuclear envelopes were not evident, but such fibrils might have been removed during Triton treatment of the nuclear membranes, or perhaps remain concealed within the dense lamina.

Morphometric analysis of pore complexes from randomly chosen nuclei was facilitated by the unique view of the nuclear surface provided by high resolution SEM. Measurements were not made at the periphery of nuclei (the tangential view distorted the dimensions in this region [Fig. 1]) but were confined to that segment of each nucleus (approximately 25%) in which all structures were clearly discernible. The results are summarized in Table I, and are compatible with published results for other mammalian cells (3, 9, 13, 17, 22, 32). Although some pore complexes might have disintegrated with Triton treatment of the nuclei, the small range of values from one nucleus to another, the few naked nuclear pores observed, and the uniformity of pattern from one region of a nucleus to another and among several nuclei argue against any significant artifact of this kind. The nonrandom distribution of nuclear pores has been confirmed in several species (30, 31, 33, 34, 47) and is evident by the clustering of the pore complexes seen in our nuclei (Figs. 5*a, b, c;* 6 *a*).

Removal of the Dense Lamina with Triton-Deoxycholate

In contrast to Triton treatment alone, 1% Triton-deoxycholate removes the dense lamina as well as the inner and outer nuclear membranes (Fig. 8). After this treatment we viewed a coarsely irregular, tufted surface punctuated by deep clefts. The surface shows no suggestion of nuclear pores or pore complexes and is distinct from the granular surface of the dense lamina. Both TEM and SEM indicate that this combination of nonionic

TABLE I

Nuclear Pore Frequency and Dimensions

A. Nuclear pore frequency in five Triton-treated nuclei (SEM at ×45,000 final magnification)

Radius		Surface area		Surface area on which pores were counted			
Nucleus r_1	Segment counted r_2	Nucleus A	Segment counted A_c	(A_c/A)	Pores counted	Pores/nucleus	Pores/μm^2 surface area
μm		μm^2		%			
2.37	2.02	71.6	16.3	23.1	210	913	12.85
2.75	2.45	95.0	25.9	27.3	295	1,092	11.49
2.51	2.04	97.2	15.7	19.8	260	1,303	14.65
2.67	2.34	89.6	23.2	25.9	327	1,257	14.12
2.80	2.30	98.5	21.1	21.5	306	1,402	14.23
Mean						1,193 ± 175	13.47 ± 1.12*

B. Nuclear pore complex dimensions

	Mean		
No. measured	Outer diameter	Annulus subunit diameter	Pore diameter
		Å	
100	848 ± 46	297 ± 33	254 ± 50

Total pore complex area = 5.65×10^{-3} μm^2 (area/pore complex) × 1,193 (mean pores/nucleus) = 6.74 μm^2. The percent of nuclear surface covered by pore complexes = 6.74 μm^2 (total pore complex area)/91.6 μm^2 (mean surface area of nucleus) = 7.3%.

* (6.7 pores/μm^2 when corrected for shrinkage.)

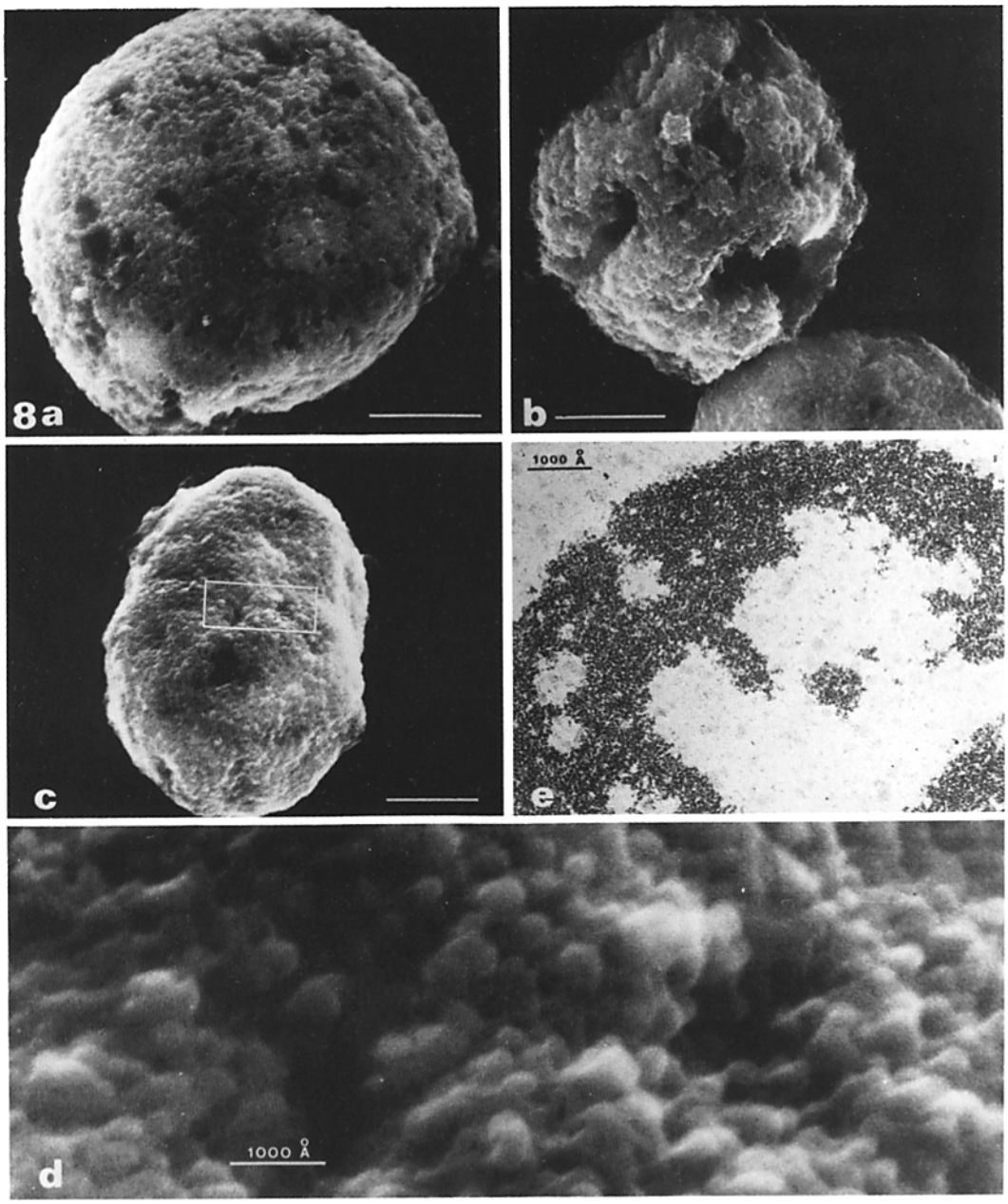

FIGURE 8 Triton-deoxycholate-treated "chromatin" nuclei. The dense lamina and pore complexes are absent. Various forms include (*a*) nucleus which has retained much of its original size and shape, (*b*) nucleus in which the chromatin has condensed considerably and from which some chromatin may be lost, (*c*) nucleus which shows considerable condensation, but in which integrity of periphery appears intact. In (*d*) a small area of Fig. 8*c* is magnified to show the tufted chromatin material which appears to be formed of a closely branched network of fibers. TEM of a nucleus (*e*), probably representing a pattern similar to that seen in Figs. 8*c*, *d*, reveals fine condensation of chromatin at the periphery of the nucleus leaving a large central clear area. Figs. 8*a-c*, bar, 1.0 μm; *a*, × 15,500; *b*, × 15,500; *c*, × 13,000; *d*, × 130,000; *e*, × 85,000.

and ionic detergents has exposed the chromatin surface. SEM further suggests that these "chromatin nuclei" in large part maintain their nuclear form in the absence of both nuclear membranes and the dense lamina. Various forms of "chromatin" nuclei are seen. Some nuclei retain much of their original size and shape and show a dispersed chromatin pattern (Fig. 8*a*). In other nuclei, the chromatin is more coarsely clumped and the integrity of the nuclear periphery is variably altered (Fig. 8*b*). A third pattern observed is that of diffuse peripheral clumping and condensation of chromatin with considerable reduction of nuclear diameter but preservation of the integrity of the periphery (Fig. 8*c*). At high magnification the exposed surfaces of such nuclei appear as closely branched networks of thick fibers with clubbed or tufted ends (Fig. 8*d*). Thin sections of many such "chromatin" nuclei indicate that nucleolar structure is altered or lost, whereas in nuclei treated with Triton X-100 alone the nucleoli are morphologically well preserved.

DISCUSSION

Technical Considerations

High resolution SEM provides a new approach to the investigation of isolated cell organelles (27–29), which correlates well with more traditional EM techniques (27). In these studies there are three areas of special concern; (*a*) attachment of sample components to the SEM support disks; (*b*) specimen shrinkage during preparation; (*c*) attainment of maximal resolution. Although nuclei of a certain size or in a particular stage of the cell cycle might not adhere to the support disks, we have no evidence to suggest this, either by SEM examination or in our correlative TEM studies. Indeed, both Triton-treated and Triton-deoxycholate-treated nuclei appear to adhere to support discs as well as intact nuclei do, mitigating against an intrinsic sampling bias. The shrinkage that occurs during specimen preparation is related largely to the critical point-drying process itself and is probably somewhat greater than that seen with thin-section and negative staining techniques (15, 22). However, our morphometric data indicate that this shrinkage is uniform throughout the sample population and among the components of individual nuclei. We also observed shrinkage similar to that seen in cell nuclei when human erythrocytes were prepared for SEM (unpublished results). Resolution is the product of several factors, including thickness of the Au-Pd coat, specimen contrast, and signal: noise ratio of the final image. We use the minimum amount of heavy metal shadow that will permit us to satisfactorily view the specimens. Although the coat thickness on planar surfaces is 50–60 Å, it is less on vertical surfaces of ribosomes and pore complex annuli, an important factor in increasing the contrast over the surface of the nuclei. When cell organelles are examined, the contrast and signal: noise ratio also improve significantly as the specimen stage is tilted, until 20–25° tilt is achieved. The biologically useful resolution, therefore, is the product of the above-mentioned factors, each of which assumes greater importance the smaller the specimen and its various components.

Nuclear Morphology

Our measurements of ribosome size and spacing on mouse liver nuclei are similar to results obtained by thin sectioning of nuclei of cement gland cells in developing embryos of *Xenopus laevis* (24), by freeze-etching of isolated nuclei from blastulae of the sea urchin *Strongylocentrotus purpuratus* (49), and to the results obtained with cytoplasmic membrane-bound ribosomes in several species (36). More important, we are able to view ribosomes over a large portion of the nuclear surface rather than in a section tangential to the surface or along the fracture face of a freeze-etched nucleus. We cannot be certain that the areas on some nuclei devoid of ribosomes represent a true dynamic state of the nucleus rather than loss of ribosomes during isolation procedures. However, those areas show no evidence of physical disruption of the membranes nor alterations in ribosomes adjacent to the naked regions. The larger size of the annular subunits of the nuclear pore complexes distinguishes them from ribosomes. We did not observe any configurations that would suggest that polysomes might emerge from nuclear pores, as has been proposed by Jacob and Danieli (24). Our assessment of possible polysome chain length is based not only on these observations but also on our experience with SEM of isolated rough endoplasmic reticulum and highly purified rat liver polysomes (reference 27; and unpublished data by R. H. Kirschner). The configuration of polysomes is difficult to judge in mouse liver nuclei because they are so densely packed. However, experiments in progress indicate that in nuclei with fewer ribosomes on their

surface the length and configuration of individual polysome chains can be determined.

By direct SEM observation, the 8 globular subunits of the pore complexes form a generally round, rather than octagonal, periphery. The fourfold symmetry that we frequently observe, both directly and by Markham rotational analysis, suggests that the annuli may consist of four paired subunits. This alternative explanation lends some support to the concept of Fabergé (10) that the nuclear pore complex can exist as an isolated free ring in one of two forms. The first is an open annulus with eight subunits; the second is a hypothetical form in which the annular ring forms a closed structure with tetragonal symmetry. Such annular complexes, however, should have a diameter only half of that of the open ring structure, a feature which we did not observe.

Several laboratories have reported the isolation of a nonmembranous nuclear envelope component, the major constituents of which are three acidic proteins of mol wt 60,000–70,000 (2, 6, 26, 37, 42). The different extraction procedures used, however, make it difficult to compare the structures obtained in one laboratory with those isolated in another. Our results with Triton-treated nuclei support the concept that in hepatocytes there is a nonmembranous lamina at the nuclear periphery to which nuclear pore complexes are attached (1, 2). These observations do not preclude the coexistence of an underlying pore-to-pore fibril network (e.g. the "nuclear ghosts" of Riley et al. [37] and Keller and Riley [26]) that might represent a skeleton within which, or upon which, the proteins of the dense lamina are deposited. Although an intramembranous pore-to-pore fibril network has been described by Scheer et al. (41), we suggest that such an intramembranous structure is probably not essential to the maintenance of nuclear shape or pore complex integrity since nuclear membranes are absent from our Triton-treated nuclei. The evidence from our Triton-deoxycholate nuclei studies further suggests that neither the dense lamina nor other structures at the nuclear periphery are necessary to maintain the integrity of the nuclear chromatin mass. Within the limits of these experiments, we cannot determine whether the physical interdigitations of the chromatin itself function to retain nuclear shape or whether this is dependent upon a "nuclear protein matrix" (or intranuclear skeletal framework), such as described by Berezney and Coffey (6).

The major role of the dense lamina, observed by SEM as a particulate structure (particle size 75–150 Å), appears to be intimately associated with the distribution, stability, and perhaps, biogenesis of the nuclear pore complexes. The dynamic aspects of nuclear pore formation (and loss) during erythrocyte maturation (21), lymphocyte stimulation (32, 33), inhibition of ATP and protein synthesis (34), and cell ischemia (8) are well established. Pore location is nonrandom (30) and it has been suggested that the organization of the underlying chromatin may determine the sites at which nuclear pores will form (3, 30). Using three criteria—alteration of heterochromatin distribution, nonrandomness (of pore distribution), and indentations in the nuclear membrane—Maul et al. (33) were able to identify prospective pore sites on the surface of cell nuclei. Many of the structures that we observe on the dense lamina of Triton-treated nuclei appear to be incompletely formed nuclear pore complexes, in the center of which we can clearly see granules of the lamina. These incomplete pore complexes, the pore complexes sharing a common subunit, and the other subunit-sized particles on the surface of the lamina possibly reflect the dynamic state of the nuclear pore complexes and their formation and dissolution in response to structural or functional alteration in the underlying chromatin. Although such double complexes as well as other particulate components resting on the dense lamina could arise through shrinkage artifact, incomplete membrane removal, or artifactual alteration of the lamina, we think this unlikely. Unfortunately, we still lack direct evidence of the site and mechanism of assembly of the annular subunits.

We thank Dr. Paul S-D. Lin and Mr. Telmer Peterson for their assistance in the use of the scanning electron microscope, and Dr. Hewson Swift for his critical review of the manuscript.

This investigation was supported in part by an award from the Ben Horwich Fund of the University of Chicago (Dr. Kirschner), and by the National Institutes of Health grant United States Public Health Service CA 12550 (Dr. Martin). The Hitachi HFS-2 SEM, located in the University of Chicago Users Microscope Laboratory, Enrico Fermi Institute, was established with a grant from the Alfred P. Sloan Foundation and is currently supported by a grant from the Biotechnology Resources Branch, NIH.

A portion of this work was presented at the 15th Annual Meeting of The American Society for Cell Biology, San Juan, Puerto Rico, 11–14 November 1975.

Received for publication 9 December 1975, and in revised form 7 September 1976.

REFERENCES

1. AARONSON, R. P., and G. BLOBEL. 1974. On the attachment of the pore complex. *J. Cell Biol.* **62:**746–754.
2. AARONSON, R. P., and G. BLOBEL. 1975. Isolation of nuclear pore complexes in association with a lamina. *Proc. Natl. Acad. Sci. U. S. A.* **72:**1007–1011.
3. ABELSON, H. T., and G. H. SMITH. 1970. Nuclear pores: the pore-annulus relationship in thin section. *J. Ultrastruct. Res.* **30:**558–588.
4. ANDERSON, T. F. 1951. Techniques for the preservation of three-dimensional structure in preparing specimens for the electron microscope. *Trans. N. Y. Acad. Sci.* **13:**130–134.
5. BARTON, A. D., W. E. KISIELESKI, F. WASSERMANN, and F. MACKEVICIUS. 1971. Experimental modification of structures at the periphery of the liver cell nucleus. *Z. Zellforsch. Mikrosk. Anat.* **115:**299–306.
6. BEREZNEY, R., and D. S. COFFEY. 1974. Identification of a nuclear protein matrix. *Biochem. Biophys. Res. Commun.* **60:**1410–1417.
7. CHAUVEAU, J., Y. MOULÉ, and C. ROUILLER. 1956. Isolation of pure and unaltered liver nuclei: morphology and biochemical composition. *Exp. Cell Res.* **11:**317–321.
8. COLEMAN, S. E., J. DUGGAN, and R. L. HACKETT. 1947. Freeze-fracture study of changes in nuclei isolated from ischemic rat kidney. *Tissue Cell.* **6:**521–534.
9. COMES, P., and W. W. FRANKE. 1970. Composition, structure and function of HeLa cell nuclear envelope. *Z. Zellforsch. Mikrosk. Anat.* **107:**240–248.
10. FABERGÉ, A. C. 1974. The nuclear pore complex: Its free existence and an hypothesis as to its origin. *Cell Tiss. Res.* **151:**403–415.
11. FAWCETT, D. W. 1966. On the occurrence of a fibrous lamina on the inner aspect of the nuclear envelope in certain cells of vertebrates. *Am. J. Anat.* **119:**129–146.
12. FELDHERR, C. M. 1972. Structure and function of the nuclear envelope. *Adv. Cell Mol. Biol.* **2:**273–307.
13. FRANKE, W. W. 1970. On the universality of nuclear pore complex structure. *Z. Zellforsch. Mikrosk. Anat.* **105:**405–429.
14. FRANKE, W. W. 1974. Structure, biochemistry, and functions of the nuclear envelope. *Int. Rev. Cytol.* **4**(Suppl.):72–236.
15. FRANKE, W. W., and U. SCHEER. 1970. The ultrastructure of the nuclear envelope of amphibian oocytes: a reinvestigation. I. The mature oocyte. *J. Ultrastruct. Res.* **30:**288–316.
16. FRANKE, W. W., and U. SCHEER. 1970. The ultrastructure of the nuclear envelope of amphibian oocytes: a reinvestigation. II. The immature oocyte and dynamic aspects. *J. Ultrastruct. Res.* **30:**317–327.
17. FRANKE, W. W., and U. SCHEER. 1974. Structures and functions of the nuclear envelope. *In* The Cell Nucleus. H. Busch, editor. Academic Press, Inc., New York. **1:**219–347.
18. GALL, J. G. 1954. Observations on the nuclear membrane with the electron microscope. *Exp. Cell Res.* **7:**197–200.
19. GALL, J. G. 1959. The nuclear envelope after $KMnO_4$ fixation. *J. Biophys. Biochem. Cytol.* **6:**115–119.
20. GALL, J. G. 1967. Octagonal nuclear pores. *J. Cell Biol.* **32:**391–399.
21. GRASSO, J. A., H. SWIFT, and G. A. ACKERMAN. 1962. Observations on the development of erythrocytes in mammalian fetal liver. *J. Cell Biol.* **14:**235–254.
22. HARRIS, J. R., M. R. PRICE, and M. WILLISON. 1974. A comparative study on rat liver and hepatoma nuclear membranes. *J. Ultrastruct. Res.* **48:**17–32.
23. HOLTZMAN, E., I. SMITH, and S. PENMAN. 1966. Electron microscopic studies of detergent-treated HeLa cell nuclei. *J. Mol. Biol.* **17:**131–135.
24. JACOB, J., and G. A. DANIELI. 1972. Electron microscope observations on nuclear pore-polysome association. *Cell Differ.* **1:**119–125.
25. KAY, R. R., and I. R. JOHNSON. 1973. The nuclear envelope: current problems of structure and of function. *Sub-Cell. Biochem.* **2:**127–166.
26. KELLER, J. M., and D. E. RILEY. 1976. Nuclear ghosts: A nonmembranous structural component of mammalian cell nuclei. *Science (Wash. D. C.).* **193:**399–401.
27. KIRSCHNER, R. H., and M. RUSLI. 1976. Identification and characterization of isolated cell organelles by high resolution scanning electron microscopy. *In* Scanning Electron Microscopy II. O. Johari and R. Becker, editors. Illinois Institute of Technology Research Institute, Chicago, Ill. 153–162.
28. KOMODA, T., and S. SAITO. 1972. Experimental resolution limit in the secondary electron mode for a field emission source scanning electron microscope. *In* Scanning Electron Microscopy. O. Johari and I. Corvin, editors. Illinois Institute of Technology Research Institute, Chicago, Ill. 129–136.
29. LIN, S-D., and M. K. LAMVIK. 1974. High resolution scanning electron microscopy at the subcellular level. *J. Microsc. (Oxf.).* **103:**249–257.
30. MARKOVICS, J., L. GLASS, and G. G. MAUL. 1974. Pore patterns on nuclear membranes. *Exp. Cell Res.* **85:**443–451.
31. MAUL, G. G. 1971. On the octagonality of the nuclear pore complex. *J. Cell Biol.* **51:**558–563.

32. MAUL, G. G., H. M. MAUL, J. E. SCOGNA, M. W. LIEBERMAN, G. S. STEIN, B. Y-L. HSU, and T. W. BORUN. 1972. Time sequence of nuclear pore formation in phytohemagglutinin-stimulated lymphocytes and in HeLa Cells during the cell cycle. *J. Cell Biol.* **55**:433–447.
33. MAUL, G. G., J. W. PRICE, and M. W. LIEBERMAN. 1971. Formation and distribution of nuclear pore complexes in interphase. *J. Cell Biol.* **51**:405–418.
34. MAUL, H. M., B. Y-L. HSU, T. M. BORUN, and G. G. MAUL. 1973. Effect of metabolic inhibitors on nuclear pore formation during the HeLa S_3 cell cycle. *J. Cell Biol.* **59**:669–676.
35. MERRIAM, R. W. 1962. Some dynamic aspects of the nuclear envelope. *J. Cell Biol.* **12**:79–90.
36. NANNINGA, N. 1973. Structural aspects of ribosomes. *Int. Rev. Cytol.* **35**:135–188.
37. RILEY, D. E., J. M. KELLER, and B. BYERS. 1975. The isolation and characterization of nuclear ghosts from cultured HeLa cells. *Biochemistry* **14**:3005–3013.
38. SADOWSKI, P. D., and J. W. STEINER. 1968. Electron microscopic and biochemical characteristics of nuclei and nucleoli isolated from rat liver. *J. Cell Biol.* **37**:147–161.
39. SCHEER, U. 1972. The ultrastructure of the nuclear envelope of amphibian oocytes. IV. On the chemical nature of the nuclear pore complex material. *Z. Zellforsch. Mikrosk. Anat.* **127**:127–148.
40. SCHEER, U. 1973. Nuclear pore flow rate of ribosomal RNA and chain growth rate of its precursor during oogenesis of *Xenopus laevis*. *Dev. Biol.* **30**:13–28.
41. SCHEER, U., J. KARTENBECK, M. F. TRENDELENBURG, J. STALLER, and W. W. FRANKE. 1976. Experimental disintegration of the nuclear envelope. Evidence for pore-connecting fibrils. *J. Cell Biol.* **69**:1–18.
42. SHELTON, K. R., C. S. COBBS, J. T. POVLISHOCK, and R. K. BURKAT. Nuclear envelope fraction proteins: Isolation and comparison with the nuclear protein of the avian erythrocyte. *Arch. Biochem. Biophys.* **174**:177–186.
43. SMITH, S. J., H. R. ADAMS, K. SMETANA, and H. BUSCH. 1969. Isolation of the outer layer of the nuclear envelope. *Exp. Cell Res.* **55**:185–197.
44. STEVENS, B. J., and J. ANDRÉ. 1969. The nuclear envelope. *In* Handbook of Molecular Cytology. A. Lima-de-Faria, editor. North-Holland Publishing Co., Amsterdam. 837–871.
45. STEVENS, B. J., and H. SWIFT. 1966. RNA transport from nucleus to cytoplasm in *Chironomus* salivary glands. *J. Cell Biol.* **31**:55–77.
46. SWIFT, H. 1958. Cytoplasmic particulates and basophilia. *In* A Symposium on the Chemical Basis of Development. W. D. McElroy and B. Glass, editors. Johns Hopkins Press, Baltimore. 174–210.
47. TIEGLER, D. J., and R. J. BAERWALD. 1972. A freeze-etch study of clustered nuclear pores. *Tissue Cell.* **4**:447–456.
48. WATSON, M. L. 1959. Further observations on the nuclear envelope of the animal cell. *J. Biophys. Biochem. Cytol.* **6**:147–156.
49. WARTIOVAARA, J., and D. BRANTON. 1970. Visualization of ribosomes by freeze-etching. *Exp. Cell Res.* **61**:403–406.
50. WISCHNITZER, S. 1973. The submicroscopic morphology of the interphase nucleus. *Int. Rev. Cytol.* **34**:1–48.